

# Initial Nucleation of Platinum Clusters after Reduction of $K_2PtCl_4$ in Aqueous Solution: A First Principles Study

Lucio Colombi Ciacchi,<sup>\*,†</sup> Wolfgang Pompe,<sup>†</sup> and Alessandro De Vita<sup>‡</sup>

Contribution from the Institut für Werkstoffwissenschaft, Technische Universität Dresden, D-01069 Dresden, Germany, Institut Romand de Recherche Numérique en Physique des Matériaux (IRRMA), Ecublens, CH-1015 Switzerland, and INFN and Dipartimento di Ingegneria dei Materiali, Università di Trieste, via A. Valerio 2, I-34100 Trieste, Italy

Received August 10, 2000. Revised Manuscript Received May 21, 2001

**Abstract:** The initial nucleation of platinum clusters after the reduction of  $K_2PtCl_4$  in aqueous solution is studied by means of first principles molecular dynamics simulations. A reaction mechanism leading to a Pt dimer is revealed both by gas-phase simulations and by simulations which model the solution environment. The key step of the observed reaction process is the formation of a Pt–Pt bond between a Pt(I) complex and an unreduced Pt(II) complex. In light of this result, we discuss the reduction process leading to the formation of platinum nanoparticles. In the generally accepted model, the nucleation of Pt particles starts only when a critical concentration of Pt(0) atoms is reached. Here, we discuss a complementary mechanism where metal–metal bonds form between Pt complexes in higher oxidation states. This is consistent with a number of experimental results which show that a high concentration of zerovalent atoms is not necessary to start the nucleation.

## I. Introduction

In the present work, the nucleation of transition metal clusters upon reduction in aqueous solution is investigated. The study focuses on the initial formation of metal–metal bonds between metal complexes immersed in the water medium. The  $PtCl_4^{2-}$  ion is chosen as a representative and widely studied example of a square-planar complex capable of producing cluster suspensions upon reduction. Platinum clusters are of special interest and are the subject of intense study, because of their unique electronic and catalytic properties.<sup>1</sup> Moreover, the nucleation and growth of Pt clusters on biopolymers can be the first step leading to the formation of metal-coated self-assembled structures.<sup>2</sup> The current knowledge of Pt cluster nucleation is based on experimental observations which only address the kinetics of the whole reduction process,<sup>3–5</sup> while a microscopic mechanism for the intermediate reaction steps is not available. The problem is considered here on the basis of theoretical modeling taken to the quantum accuracy level, as made possible by recent advances in ab initio techniques and by the use of massively parallel computing. In particular, we attempt for the first time a direct simulation of metal–metal bond formation between two complexes in the water medium using first-

principles molecular dynamics (FPMD) techniques. The nucleation of Pt clusters on a DNA substrate will be addressed in a forthcoming work.<sup>6</sup> Here, we investigate the homogeneous nucleation process which takes place in standard reduction experiments.

A method for preparing stable colloidal dispersions of platinum particles was proposed in a classic paper by Rampino and Nord in the 1940s<sup>7</sup> and is still widely employed. The preparation is quite simple: a Pt(II) or Pt(IV) salt is dissolved in water, the solution is aged overnight, and a reducing agent is then added to the solution. This causes the precipitation of platinum colloids after a time which strongly depends on the reactants used and on a few other reaction parameters such as pH and temperature. The presence of a stabilizing polymer in the reduction bath is generally needed to prevent the agglomeration of the metal particles.<sup>7</sup> A main goal in colloid chemistry is to achieve good control of the particle size and shape, since these determine the catalytic efficiency of the colloidal dispersion.<sup>8,9</sup> At the same time, the preparation of metal catalysts is a delicate process: extremely pure reactants and solvents are, e.g., required to obtain colloidal suspensions of good quality. Thus, the growth of platinum clusters in the presence of different reducing agents and stabilizing polymers has been the object of numerous detailed experimental studies.<sup>3–5,7–14</sup> The radiation-

<sup>†</sup> Technische Universität Dresden.

<sup>‡</sup> IRRMA and Università di Trieste.

(1) Schmid, G. *Cluster and Colloids*; VCH: Weinheim, 1994. In particular, Chapter 6, by J. S. Bradley, is dedicated to the chemistry of transition metal colloids and contains a rich reference list.

(2) Braun, E.; Eichen, Y.; Sivan, U.; Ben-Yoseph, G. *Nature* **1998**, *391*, 775–778. Richter, J.; Seidel, R.; Kirsch, R.; Mertig, M.; Pompe, W.; Plaschke, J.; Schackert, H. K. *Adv. Mater.* **2000**, *12*, 507–510. Mertig, M.; Kirsch, R.; Pompe, W.; Engelhardt, H. *Eur. Phys. J. D* **1999**, *9*, 45–48. Kirsch, R.; Mertig, M.; Pompe, W.; Wahl, R.; Sadowsky, G.; Böhm, K. J.; Unger, E. *Thin Solid Films* **1997**, *305*, 248–253.

(3) Henglein, A.; Giersig, M. *J. Phys. Chem. B* **2000**, *104*, 6767–6772.

(4) Henglein, A.; Ershov, B. G.; Malow, M. *J. Phys. Chem.* **1995**, *99*, 14129–14136.

(5) Duff, D. G.; Edwards, P. P.; Johnson, B. F. G. *J. Phys. Chem.* **1995**, *99*, 15934–15944.

(6) Mertig, M.; Colombi Ciacchi, L.; Seidel, R.; Pompe, W.; De Vita, A. In preparation.

(7) Rampino, L. D.; Nord, F. F. *J. Am. Chem. Soc.* **1941**, *63*, 2745–2749.

(8) Turkevich, J.; Kim, G. *Science* **1970**, *169*, 873–879.

(9) Ahmadi, T. S.; Wang, Z. L.; Green, T. C.; Henglein, A.; El-Sayed, M. A. *Science* **1996**, *272*, 1924–1926.

(10) Toshima, N.; Nakata, K.; Kitoh, H. *Inorg. Chim. Acta* **1997**, *265*, 149–153.

(11) Mizukoshi, Y.; Oshima, R.; Maeds, Y.; Nagata, Y. *Langmuir* **1999**, *15*, 5, 2733–2737.

(12) Schmid, G.; Harms, M.; Malm, J.-O.; Bovin, J.-O.; van Ruitenbeck, J.; Zandbergen, H. W.; Fu, W. T. *J. Am. Chem. Soc.* **1993**, *115*, 2046–2048.

induced nucleation of metal clusters has been investigated at the atomic scale in the case of silver and other monovalent ions.<sup>15</sup> However, the specific mechanism through which platinum colloids nucleate and start growing is still not clear.<sup>15</sup> The generally made assumption (explicit or implicit) is that the Pt(II) or Pt(IV) complexes first react with the reducing agent to give isolated Pt(0) atoms. After a while, when a critical concentration of Pt(0) atoms is reached, metal clusters start forming at an appreciable rate<sup>5,10,11,14</sup> by aggregation of these atoms. It should be noted that no direct evidence of the isolated Pt(0) atoms has ever been presented. The presence of Pt(0) atoms is generally inferred from the kinetics of the whole reduction process.<sup>5</sup> In another proposed mechanism, the reaction could involve a metallorganic precursor, in which many metal ions are chemically bound to the reducing agent in a polymeric structure. This mechanism was postulated for the first time in the case of the reduction of  $\text{AuCl}_4^-$  to colloidal gold by citrate.<sup>16</sup> However, the presence of a metallorganic intermediate has been shown to be generally not necessary.<sup>5</sup>

On the other hand, some experimental observations indicate the possibility of forming metal–metal bonds before the critical concentration of zerovalent atoms is reached. In a recent accurate analysis of the reduction kinetics of  $\text{PtCl}_4^{2-}$  with hydrogen, monovalent platinum has been postulated to be the first reaction intermediate.<sup>3</sup> In the same work, the appearance of free Pt(0) atom intermediates has been excluded.<sup>3</sup> In addition, clusters composed of few metal atoms, sometimes in oxidation states higher than zero, have been produced with methods that differ from the standard preparation of colloids only by the presence of ligand molecules such as carbonyls or phosphines in the solution.<sup>1</sup> An intriguing example is the production of Pt(I) dimers in a concentrated HCl solution by reduction of  $\text{K}_2\text{PtCl}_4$  with CO,<sup>17</sup> due either to a reaction between partially reduced Pt(I) complexes or to a comproportionation between unreduced Pt(II) and reduced Pt(0) complexes.<sup>18</sup> We note that this is direct evidence that the formation of metal–metal bonds between platinum complexes in reduction baths does not necessarily involve zerovalent atoms only.

This is also the case when silver particles start growing in the initial stage of the reduction/nucleation process. After radiolytic reduction of  $\text{Ag}^+$ ,  $\text{Ag}(0)$  atoms have been observed to aggregate to monovalent  $\text{Ag}^+$  ions to form  $\text{Ag}_2^+$  dimers.<sup>15</sup> Successive coalescence and reduction steps finally lead to colloidal particles. Interestingly, the addition of ions to a growing cluster takes place before their reduction to the metallic state. Reduction happens only later and involves the whole cluster.<sup>15</sup> In the case of platinum, colloids are produced via a chain reaction in which the first formed clusters catalyze the further reduction of the metal complexes still present in solution.<sup>3,4</sup> The autocatalytic process starts at the very beginning of the reaction, when only very few complexes are reduced. In this case, one does not have to wait the induction time necessary to reach a critical concentration of zerovalent atoms, as in the standard nucleation mechanism. This suggest that dimerization may

happen in the first step of cluster growth before both metal atoms are reduced to Pt(0), similar to the case of Ag.

In this work, we explore the problem of the initial nucleation of platinum particles taking into account this possibility. In other words, we look for a mechanism of forming Pt–Pt bonds upon reduction of Pt(II) complexes in solution, without assuming the prior complete reduction of both Pt atoms to their zerovalent state. To reach this goal, we investigate the initial nucleation of platinum clusters in a series of FPMD simulations. Among the Pt(II) salts, we assume as starting point the widely used  $\text{K}_2\text{PtCl}_4$ . The reduction of Pt(II) to its metallic state can be obtained by electron transfer from inorganic and organic reducing agents, via photodecomposition,<sup>10</sup> radiolysis,<sup>4</sup> sonochemical reduction,<sup>11</sup> and a variety of other methods.<sup>1</sup> Given this variety of agents and techniques, no attempt has been made to model any particular reduction process. Since the presence of a stabilizer is not directly necessary for the reduction (while it helps to control the size and shape of the metal particles<sup>9</sup>), stabilizers are also not directly addressed in this study. Our FPMD simulations are performed on systems which include Pt complexes only and contain from the start the number of electrons which is appropriate to the desired reduction state.

The computational technique and the simulation parameters are briefly described and tested on simple molecules in the next section. The FPMD simulations are described in section III and discussed in section IV. Finally, a summary is given in section V.

## II. Computational Method and Test Calculations

Our electronic and structural optimizations, as well as the FPMD simulations, are performed using the Car–Parrinello (CP) method<sup>19</sup> in the framework of the spin-polarized density functional theory (DFT).<sup>20</sup> The gradient-corrected exchange–correlation energy is described by the functional proposed in ref 21, implemented with the technique of ref 22. Periodic boundary conditions are used. The Bloch functions and the electron density are expanded on a plane-wave basis set up to a kinetic energy cutoff of 60 and 240 Ry, respectively. Only valence Bloch electrons at the  $\Gamma$  point of the Brillouin zone are considered, and separable norm-conserving pseudopotentials<sup>23</sup> are used to model their interaction with the core ions. The pseudopotentials have been constructed with the program fhi98PP following the scheme of ref 24. In particular, the Pt pseudopotential is generated for the neutral atom considering 18 valence electrons in the configuration  $5s^25p^65d^{9.95}6s^{0.05}$ , the core radius for all three components is 1.60 au, and the p component is taken to be local.<sup>25</sup> The accuracy of this pseudopotential is tested for the  $\text{PtCl}_4^{2-}$  ion and the bare Pt dimer. The computed Pt–Cl bond length in  $\text{PtCl}_4^{2-}$  is 2.35 Å, which compares well with the experimental value of 2.34 Å<sup>26</sup> and with the value 2.35 Å of a previous calculation<sup>27</sup> based on similar techniques. The electronic configuration of minimal energy for the bare neutral platinum dimer is found to be a triplet, whereas the singlet energy level is found 0.5 eV higher. The Pt–Pt bond length in the dimer is 2.38 Å, to be compared with other theoretical

(19) Payne, M. C.; Teter, M. P.; Allan, D. C.; Arias, T. A.; Joannopoulos, J. D. *Rev. Mod. Phys.* **1992**, *64*, 1045–1097. Car, R.; Parrinello, M. *Phys. Rev. Lett.* **1985**, *55*, 2471–2474.

(20) Gunnarsson, O.; Lundqvist, B. I. *Phys. Rev. B* **1976**, *13*, 4274–4298.

(21) Perdew, J. P.; Wang, Y. *Phys. Rev. B* **1992**, *45*, 13244–13249.

(22) White, J. A.; Bird, D. M. *Phys. Rev. B* **1994**, *50*, 4954–4957.

(23) Troullier, N.; Martins, J. L. *Phys. Rev. B* **1991**, *43*, 1993–2006.

(24) Fuchs, M.; Scheffler, M. *Comput. Phys. Commun.* **1999**, *119*, 67–98.

(25) Kleinman, L.; Bylander, D. M. *Phys. Rev. Lett.* **1982**, *48*, 1425–1428.

(26) Atoji, M.; Ritchardson, J. W.; Rundle, R. E. *J. Am. Chem. Soc.* **1957**, *79*, 3017–3020.

(27) Carloni, P.; Andreoni, W.; Hütter, J.; Curioni, A.; Giannozzi, P.; Parrinello, M. *Chem. Phys. Lett.* **1995**, *234*, 50–56.

(13) Van Rheeën, P. R.; McKelvy, M. J.; Glaunsinger, W. S. *J. Solid State Chem.* **1987**, *67*, 151–169.

(14) Kraeutler, B.; Bard, A. J. *J. Am. Chem. Soc.* **1978**, *100*, 4137–4138.

(15) Belloni, J.; Mostafavi, M. In *Metal Clusters in Chemistry*; Braunstein, P., Oro, L. A., Raithby, P. R., Eds.; Wiley-VHC: New York, 1999; pp 1213–1247.

(16) Turkevich, J.; Stevenson, P. C.; Hillier, J. *J. Discuss. Faraday Soc.* **1951**, *11*, 55–75.

(17) Gogging, P. L.; Goodfellow, R. J. *J. Chem. Soc., Dalton Trans.* **1973**, 2355–2359.

(18) Müller, T. E.; Ingold, F.; Menzer, S.; Mingos, D. M. P.; Williams, D. *J. Org. Chem.* **1997**, *528*, 1163–178.

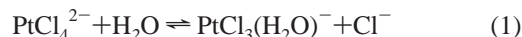
DFT values of 2.39 Å<sup>28</sup> and 2.40 Å.<sup>29</sup> This is in reasonable agreement with the experimental value of 2.45 Å measured by STM techniques on a graphite support.<sup>30</sup> Our computed binding energy for the dimer is 3.34 eV, which should be compared with the theoretical values of 2.44 eV<sup>28</sup> and 3.30 eV<sup>29</sup> and with the reported experimental values which lie in a range between 2.80 and 3.71 eV.<sup>30</sup>

In the FPMD simulations, the mass of hydrogen is increased to 2.0 amu, the fictitious electronic mass in the CP method is set to 1100 au, and a time step of 6.0 au (about 0.145 fs) is used. These parameters are adequate for CP dynamical simulations of aqueous systems.<sup>31</sup> When necessary, control of the temperature is achieved by a Nose–Hoover thermostat<sup>32</sup> or simply by scaling the atomic velocities. All calculations were performed on the massively parallel CRAY-SGI computer platforms of the Center for High Performance Computing at the Dresden University of Technology, using the LAUTREC code.<sup>33</sup>

### III. Results

We report here our results, following the steps which lead to the formation of platinum dimers upon reduction of Pt(II) complexes. The starting point is a water solution of  $K_2PtCl_4$ . The solvolysis products are then exposed to a reducing agent. As mentioned earlier, we do not attempt here to investigate the electron-transfer mechanism from a specific reducing agent to a Pt(II) complex. Rather, the reducing electron is added each time into the simulation cell containing one or more Pt complexes, assuming that a good model for the system immediately after reduction can be obtained this way after electronic optimization and MD equilibration. This “vertical addition” of an electron to the system followed by ionic motion in the presence of an extra charge may be linked to what happens in radiolytic reduction processes. Here the electrons produced by  $\gamma$ -ray irradiation of the platinum salt solution can be thought to fall into the LUMO states of the metal complexes<sup>4,11,15</sup> present in the solution. More generally, we can address in this way all those processes where the reducing agent has only the instrumental role of electron donor, beside which its exact character is little relevant to the subsequent evolution of the reduced fragment. It would seem reasonable to assume that this is the case in many reduction processes involving Pt complexes. We note that in the experiments the final reduction product of a platinum salt is essentially always an ensemble of metal crystallites with diameters ranging between 2 and 3 nm, despite the great number of possible reducing agents. Different size distributions of the metal particles in the colloidal suspension are due only to more or less marked aggregation of the crystallites (Pt clusters bigger than 3 nm are rarely single crystals<sup>13</sup>). Finally, modifications of the colloid morphology are mainly due to different concentrations and types of protective agents<sup>9</sup> and again do not depend on the reducing agent used.

**A. Solvolysis Products of  $K_2PtCl_4$  in Water Solution.** After the dissociation of  $K_2PtCl_4$ , the  $PtCl_4^{2-}$  ions undergo the following solvolysis reactions:<sup>34</sup>



At equilibrium, a 1 mM solution of  $K_2PtCl_4$  consists of 5%  $PtCl_4^{2-}$ , 53%  $PtCl_3(H_2O)^-$ , and 42%  $PtCl_2(H_2O)_2$ .<sup>35</sup> The aging time necessary for reaching the equilibrium is about 1 day at room temperature. The solution is then stable for some days. After that, decomposition of the complexes starts being noticeable.<sup>34</sup> We calculated the relaxed geometries and the electronic structure of the three Pt(II) complexes in the gas phase, using a repeated cubic supercell with edge 20 Å. The optimized bond lengths and angles of the molecules and the Kohn–Sham eigenvalues are reported in Table 1 and in the scheme of Figure 1, respectively. The vertical electronic affinities (VEAs) of the three complexes are computed as the change in total energy upon addition of one electron to the system, at fixed atomic positions. We note that because of the periodic boundary conditions used, the total energies of charged systems must be evaluated including appropriate corrective terms.<sup>36,37</sup> We do not take into account the contribution to the electron affinity given by the variation of zero-point vibration energy upon the reduction, since these zero-point corrections are generally smaller than the systematic errors due to other approximations (e.g., the use of pseudopotentials). Our computed EAs for the Cl and O atoms are 3.6 and 1.6 eV (experimental, 3.6 and 1.5 eV,<sup>38</sup> respectively). For the relaxed Pt<sub>2</sub> dimer we obtain an EA of 1.7 eV (experimental, 1.9 eV<sup>38</sup>). Of the three Pt(II) complexes, only the neutral complex  $PtCl_2(H_2O)_2$  binds an extra electron, giving a positive calculated VEA of 0.7 eV. The reducing electron remains instead delocalized in the case of the negatively charged complexes  $PtCl_4^{2-}$  and  $PtCl_3(H_2O)^-$ .<sup>39</sup>

**B. Reduction of  $PtCl_2(H_2O)_2$ .** We now turn to the study of  $PtCl_2(H_2O)_2$  upon addition of one electron. We first minimize the electronic structure at fixed atoms. The calculated energy levels for both spin manifolds with respect to the position of the HOMO-1 state are reported in Figure 1 (right). The atoms are then allowed to move. We report in Figure 2 the evolution of the particle density associated with the singly occupied orbital during the dynamics. This is obtained as the difference  $\rho_{\uparrow} - \rho_{\downarrow}$  of the electron densities  $\rho_{\uparrow}$ ,  $\rho_{\downarrow}$  associated with the “up” and “down” spin manifolds. At the beginning of the run, the additional electron falls as expected into the  $d_{z^2-y^2}$  LUMO orbital of the neutral square-planar  $PtCl_2(H_2O)_2$ . However, within  $\sim 100$  fs, the two water ligands dissociate from the complex. At this point, the Cl–Pt–Cl angle starts increasing from the initial value of about 100°. Within  $\sim 0.2$  ps the angle reaches 180° and a linear  $PtCl_2^-$  complex is formed, which is then stable in the time scale of the simulation. After quenching the atomic motion, the Pt–Cl distance is 2.25 Å, i.e., only 0.02 Å smaller than the initial value in the  $PtCl_2(H_2O)_2$  complex. In  $PtCl_2^-$ , the Pt atom has the exotic  $d^9$  electron configuration, and a  $d^{10}$  Pt(0) complex is readily obtained when the reduction is completed by adding one more electron. The  $PtCl_2^{2-}$  complex is also linear, with a Pt–Cl bond length increased to 2.32 Å. The five highest occupied molecular orbitals of this complex are shown in Figure

(28) Cui, Q.; Musaev, D. G.; Morokuma, K. *J. Chem. Phys.* **1998**, *108*, 8418–8428.

(29) Yang, S. H.; Drabold, D. A.; Adams, J. B.; Ordejón, P.; Glassford, K. *J. Phys.: Condens. Matter* **1997**, *9*, L39–L45.

(30) Gupta, S. K.; Nappi, B. M.; Gingerich, K. A. *Inorg. Chem.* **1981**, *20*, 966–969. Miedema, A. R.; Gingerich, K. A. *J. Phys. B* **1979**, *12*, 2081–2095.

(31) Sprick, M.; Hütter, J.; Parrinello, M. *J. Chem. Phys.* **1996**, *105*, 1142–1152.

(32) Nose, S. *Mol. Phys.* **1984**, *52*, 255–268. Hoover, W. G. *Phys. Rev. A* **1985**, *31*, 1695–1697.

(33) De Vita, A.; Canning, A.; Car, R. *EPFL Supercomput. J.* **1994**, *6*, 22–27.

(34) Sanders, C. I.; Martin, D. S., Jr. *J. Am. Chem. Soc.* **1961**, *83*, 807–810.

(35) Cotton, F. A.; Wilkinson, G.; Murillo, C. A.; Bochmann, M. *Advanced Inorganic Chemistry*, 6th ed.; John Wiley: New York, 1999.

(36) Leslie, M.; Gillan, M. J. *J. Phys. C* **1985**, *18*, 973–982.

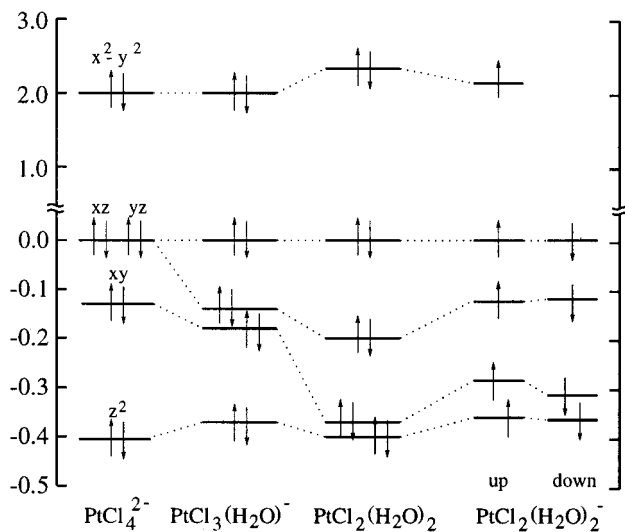
(37) Makov, G.; Payne, M. C. *Phys. Rev. B* **1995**, *51*, 4014–4022.

(38) Lide, D. R., Ed. *CRC Handbook of Chemistry and Physics*; CRC Press: Boca Raton, FL, 1996.

(39) The electron added to investigate a possible reduction state remains delocalized also if the space surrounding  $PtCl_4^{2-}$  or  $PtCl_3(H_2O)^-$  in the simulation cell is filled with water molecules, to model the solution environment.

**Table 1.** Optimized Bond Lengths (Å) and Angles of the Square-Planar Complexes Described in Section IIIA

	Pt <sub>2</sub> Cl <sub>4</sub> <sup>2-</sup>	PtCl <sub>3</sub> (H <sub>2</sub> O) <sup>-</sup>	PtCl <sub>2</sub> (H <sub>2</sub> O) <sub>2</sub>
Pt–Cl	2.35	2.32, 2.27	2.27
Pt–O		2.10	2.13
Cl–Pt–Cl	90.0°	94.7°	99.0°
Cl–Pt–O		85.3°	80.8°
O–Pt–O			99.5°

**Figure 1.** Kohn–Sham energy levels (eV) of three square-planar Pt complexes near the HOMO–LUMO gap. The local spin density spectrum of the open-shell reduced complex PtCl<sub>2</sub>(H<sub>2</sub>O)<sub>2</sub><sup>-</sup> is also shown (see text).

3. The  $\pi_g$  symmetry of the degenerate HOMOs corresponds to that of the singly occupied orbital of PtCl<sub>2</sub><sup>-</sup> (cf. Figure 2c). A  $\sigma_g$  orbital derived from the atomic 5d<sub>z<sup>2</sup></sub> corresponds to an energy level located  $\sim 0.5$  eV below the HOMO level. As an independent check on these results, the electronic structure of PtCl<sub>2</sub><sup>2-</sup> was computed again using a Gaussian basis set and without imposing periodic boundary conditions.<sup>40–44</sup> The calculation led to the same sequence in the orbital symmetries shown in Figure 3. Finally, the linear PtCl<sub>2</sub><sup>2-</sup> complex was obtained also as the final configuration of a separate FPMD run in which the two extra electrons are added to the PtCl<sub>2</sub>(H<sub>2</sub>O)<sub>2</sub> at the same time at the beginning of the simulation.

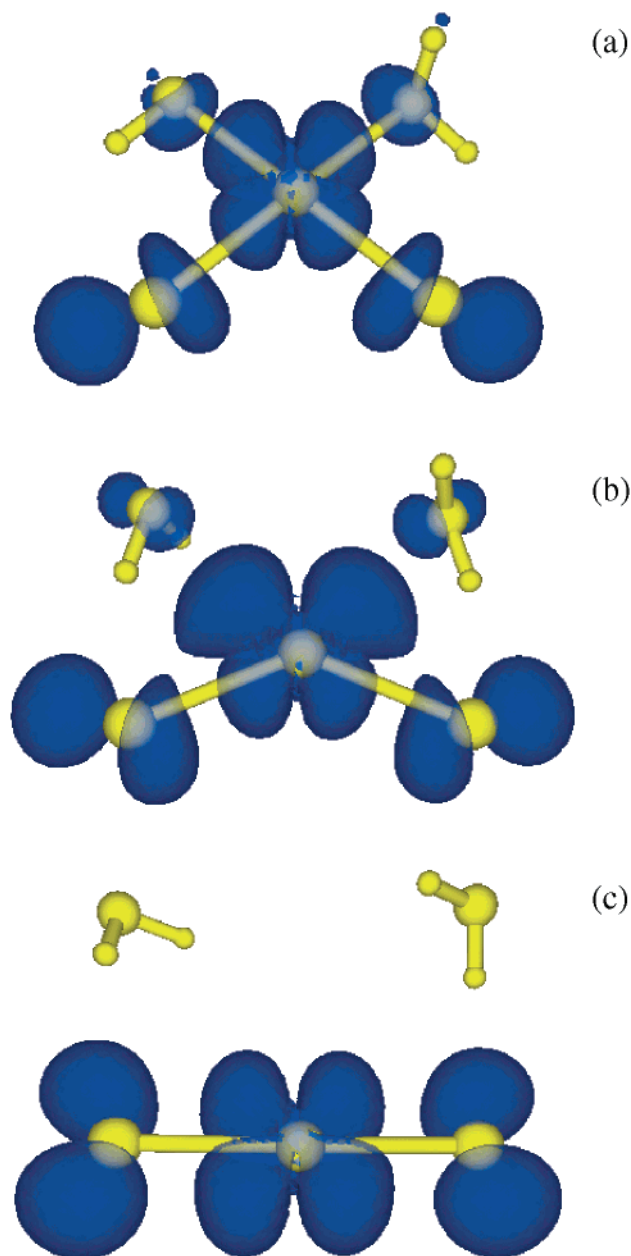
(40) Frisch, M. J.; Trucks, G. W.; Schlegel, H. B.; Scuseria, G. E.; Robb, M. A.; Cheeseman, J. R.; Zakrzewski, V. G.; Montgomery, J. A.; Stratmann, R. E.; Burant, J. C.; Dapprich, S.; Millam, J. M.; Daniels, A. D.; Kudin, K. N.; Strain, M. C.; Farkas, O.; Tomasi, J.; Barone, V.; Cossi, M.; Cammi, R.; Mennucci, B.; Pomelli, C.; Adamo, C.; Clifford, S.; Ochterski, J.; Petersson, G. A.; Ayala, P. Y.; Cui, Q.; Morokuma, K.; Malick, D. K.; Rabuck, A. D.; Raghavachari, K.; Foresman, J. B.; Cioslowski, J.; Ortiz, J. V.; Stefanov, B. B.; Liu, G.; Liashenko, A.; Piskorz, P.; Komaromi, I.; Gomperts, R.; Martin, R. L.; Fox, D. J.; Keith, T.; Al-Laham, M. A.; Peng, C. Y.; Nanayakkara, A.; Gonzalez, C.; Challacombe, M.; Gill, P. M. W.; Johnson, B. G.; Chen, W.; Wong, M. W.; Andres, J. L.; Head-Gordon, M.; Replogle, E. S.; Pople, J. A. *Gaussian 98*, Revision A.2; Gaussian, Inc., Pittsburgh, PA, 1998.

(41) We used a SDD valence triple- $\zeta$  basis set<sup>42</sup> together with the corresponding Stuttgart/Dresden pseudopotential for the description of core electrons for the Pt atoms, and a D95 Dunning/Huzinaga valence double- $\zeta$  basis set<sup>43</sup> for the remaining atoms. The BPW91 exchange correlation functional<sup>44</sup> was used.

(42) Leininger, T.; Nicklass, A.; Stoll, H.; Dolg, M.; Schwerdtfeger, P. *J. Chem. Phys.* **1996**, *105*, 1052. (Web address: <http://theochem.uni-stuttgart.de/pseudopotentials>)

(43) Dunning, T. H., Jr.; Hay, P. J. In *Modern Theoretical Chemistry*; Schaefer, H. F., III, Ed.; Plenum: New York, 1976; pp 1–28.

(44) Perdew, J. P. In *Electronic Structure of Solids '91*; Ziesche, P., Eschrig, H., Eds.; Akademie Verlag: Berlin, 1991. Becke, A. D. *Phys. Rev. A* **1988**, *38*, 3098–3100.

**Figure 2.** Evolution of PtCl<sub>2</sub>(H<sub>2</sub>O)<sub>2</sub> upon addition of one reducing electron (gas-phase reaction). The particle density associated with the unpaired electron is depicted as isovalue surface at 0.002 au.

To investigate the effect of the solution environment on the reduction process, we fill the empty space surrounding the Pt complex with water molecules at bulk water density. The simulated system contains a PtCl<sub>2</sub>(H<sub>2</sub>O)<sub>2</sub> complex and 46 water molecules in a repeated cubic cell of edge 12 Å. The system is first equilibrated for 0.5 ps in a constant temperature (CT) simulation at 300 K, and then the reduction is promoted by adding one electron to the system. After minimization of the electronic structure at fixed ionic positions, the dynamics at 300 K is continued. The same pattern of events observed in the gas-phase simulation is obtained here in solution, although the rearrangement of the complex is slowed by the steric hindrance of the surrounding water solution. Namely, the square-planar symmetry of the complex is soon broken by the successive loss of the two water ligands. Once more, the chlorine atoms move off the initial cis geometry, and in less than 2 ps of simulated time a linear PtCl<sub>2</sub><sup>-</sup> complex is obtained, which remains stable on the time scale of the simulation. Further reduction from this

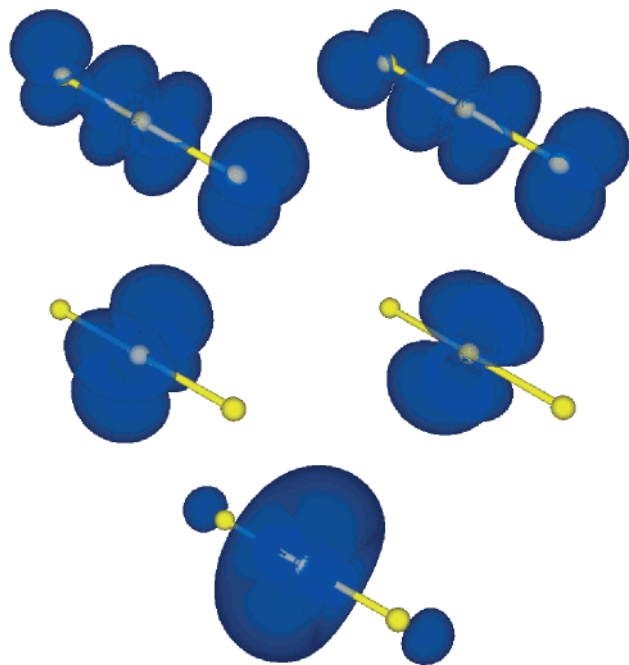


**Figure 3.** Five highest occupied molecular orbitals of  $PtCl_2^{2-}$  (isodensity surfaces at 0.003 au). Top rank: the two  $\pi_g$  degenerate HOMOs. Middle rank: the two degenerate  $\delta_g$  orbitals (their energy level is located  $\sim 0.3$  eV below the HOMO level). Bottom rank:  $\sigma_g$  orbital (energy level located  $\sim 0.5$  eV below the HOMO level).

point leads to the  $PtCl_2^{2-}$  complex. Also in this case the complex remains stable, no hydrolysis occurring in 2.5 ps of simulated time.

**C. Formation of a Platinum Dimer in Water.** With the aim of investigating the formation of a Pt–Pt bond upon reduction of platinum salt in solution, we perform MD simulations on a system of two Pt(II) complexes and 36 water molecules contained in a repeated cubic cell of edge 12 Å (Figure 4a). The system is first annealed at 300 K for 1.25 ps, after which the Pt–Pt distance is  $\sim 7$  Å, and then one electron is added and the dynamics is continued. The analysis of the electron density reveals that the additional electron immediately localizes in the LUMO state of one of the two square-planar complexes, which is thus reduced to contain a Pt(I) atom. Once more, in less than 2 ps of further simulation time a linear  $PtCl_2^-$  develops from this reduced complex after the loss of both water ligands (Figure 4b). Remarkably, letting the system evolve after this stage, we observe the formation of a Pt–Pt bond between the linear Pt(I) complex and the square-planar Pt(II) complex left intact by the reduction (Figure 4c). The Pt(I)–Pt(II) dimer then remains stable for 2 ps more, after which the simulation is stopped. After quenching of the atomic motion, the equilibrium Pt–Pt distance is found to be 2.9 Å. During the dimer formation, the water molecules rearrange so that some empty space is present in the cell at the end of the simulation. This happens because the excluded volume defined by the final  $Pt_2$  complex is significantly smaller than that associated with the two isolated square-planar complexes. To ensure that the observed reaction is not dependent on the lack of water, we performed a novel simulation introducing 10 more water molecules in the system, therefore containing 46 water molecules, a  $PtCl_2(H_2O)_2$  complex, and a linear  $PtCl_2^-$  complex. The Pt atom of the linear Pt(I) complex was placed on the  $z$  axes of the square-planar Pt(II) complex, with its two  $Cl^-$  ligands on top positions with respect to a  $Cl^-$  ligand and an  $H_2O$  ligand of the square-planar complex.

The initial distance between the Pt atoms of the two complexes was set to 4.8 Å. The simulation led as before to the formation of a bond between the platinum atoms. To investigate if the observed bond formation process is affected by the initial value of the twist angle between the two complexes, we performed two more FPMD simulations of a system containing a Pt(I) complex, a Pt(II) complex, and 37 randomly placed water molecules, setting the initial Pt–Pt distance to 4.0 Å. In these simulations, the initial torsion angle defined by the two Pt atoms and two  $Cl^-$  ligands (one per Pt atom) was varied by  $+45^\circ$  and  $-45^\circ$  with respect to the value used for the 46 water molecule system in the previous simulation. Both simulations led, as before, to the formation of a Pt–Pt bond of equilibrium length 2.9 Å.

Finally, we add a second reducing electron to the annealed configuration of the Pt(I)–Pt(II) dimer surrounded by 36 water molecules, and start a FPMD-CT simulation at 300 K from this point. In this case, a chlorine ligand is immediately lost, and the structure of the dimer gradually changes so that after about 1.5 ps the Pt–Pt bond is in the same plane of the bonds with the other ligands for both Pt atoms (Figure 4d). The angle between the two ligand planes is  $\sim 75^\circ$ . The final geometry resembles very closely that of the  $[Pt_2Cl_4(CO)_2]^{2-}$  ion, as obtained by reduction of  $K_2PtCl_4$  with CO.<sup>17,45</sup> The Pt–Pt equilibrium distance is 2.6 Å, which is a typical value for Pt(I) dimers.<sup>18</sup>

**D. Characterization of the Pt–Pt Bond.** To understand the mechanism of bond formation leading to the Pt(I)–Pt(II) dimer, we perform a series of electronic structure minimizations on fixed gas-phase atomic geometries. Our purpose is to isolate the evolution of the particle density associated with the unpaired electron during the bond formation (Figure 5a–d). The geometry of the two Pt complexes is extracted from the system shown in Figure 4b, and the Pt–Pt distance is varied by moving the complexes by successive rigid translations. When the  $PtCl_2^-$  molecule is far from  $PtCl_2(H_2O)_2$  (Figure 5a), the isolated electron occupies the  $\pi_g$  orbital, as expected (cf. Figure 2c). When the Pt–Pt distance is reduced to about 4 Å, the  $\sigma_g$  energy level (cf. Figure 3) becomes higher than the  $\pi_g$  one and is thus the one occupied by the unpaired electron (Figure 5b). At this point we observe hybridization between the  $\sigma_g$  orbital and the occupied  $d_{z^2}$  state of  $PtCl_2(H_2O)_2$  (Figure 5b,c), indicating the formation of a bond. The fully relaxed structure of the Pt(I)–Pt(II) dimer with the antibonding half-filled HOMO state is shown in Figure 5d, and the atomic coordinates are reported in Table 2. In the gas-phase, the Pt–Pt equilibrium distance is 2.87 Å. The analysis of the electron density of the formed dimer in the equilibrium structure reveals the existence of a bond critical point between the Pt atoms (Figure 6), as should be the case if a Pt–Pt chemical bond is present. Our computed binding energy for the Pt(I)–Pt(II) dimer system is 1.52 eV, obtained as the difference between the total energy of the dimer system in the gas phase and the sum of the energies of the two isolated complexes.<sup>46</sup> A further optimization of the Pt(I)–Pt(II) dimer structure was performed as an additional check, using a Gaussian

(45) Modinos, A.; Woodward, P. J. *Chem. Soc., Dalton Trans.* **1975**, 1516–1520.

(46) The computed total energies of charged systems must be corrected for the spurious electrostatic interactions induced by the periodic boundary conditions adopted in the plane-wave formalism. A simple way to compute the correction terms up to order  $O(L^{-4})$  in the case of cubic supercells of edge-length  $L$  is reported in refs 36 and 37. We note that in our computation the total energy values depend strongly on the instantaneous configuration of the water molecules surrounding the complex, so that computing a reliable binding energy in the water environment would be a much more difficult task.

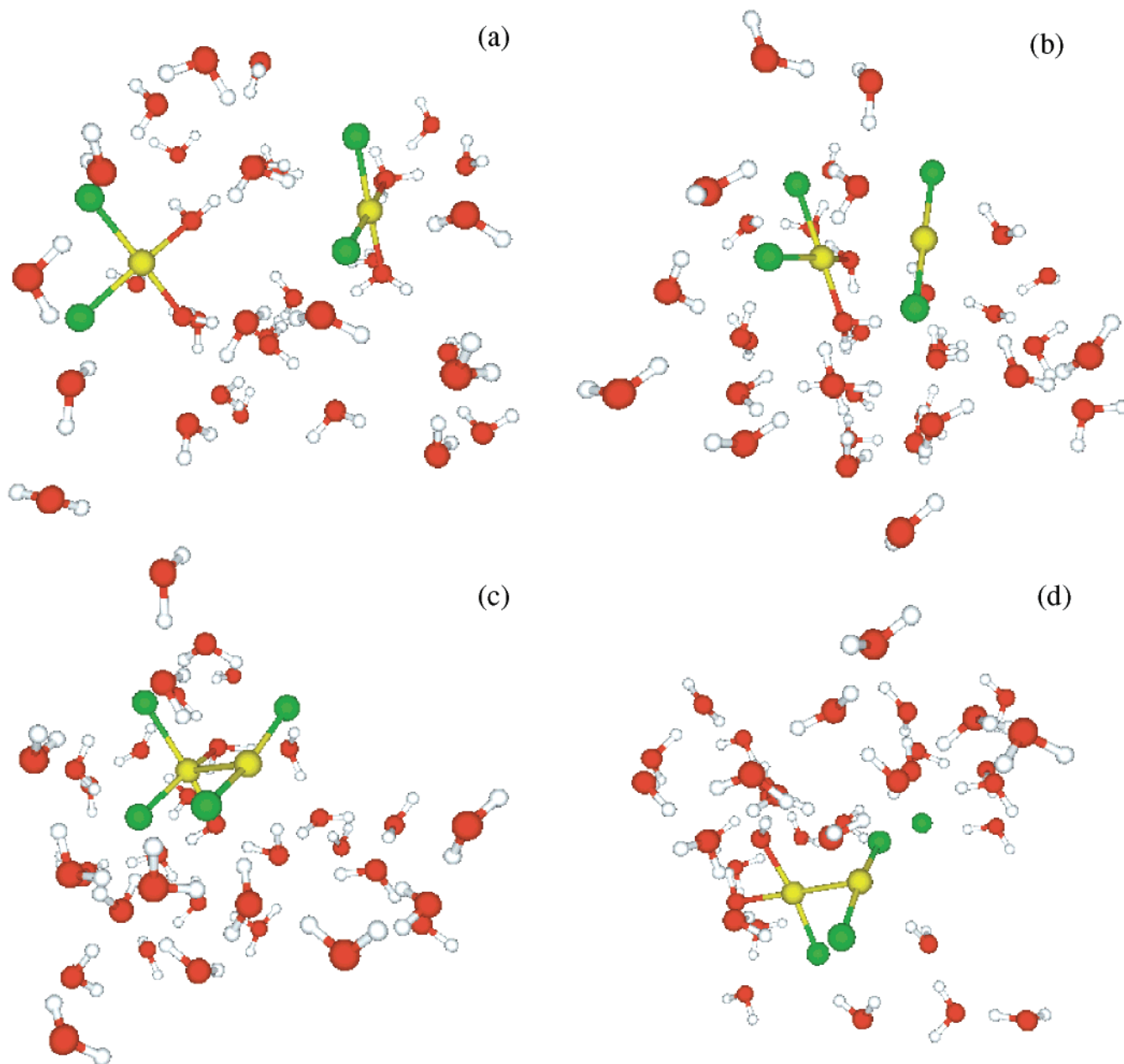


**Figure 4.** Snapshots from FPMD simulations showing the formation of a Pt dimer from two Pt(II) complexes (see text, section IIIC): (a) Two Pt(II) complexes surrounded by 36 water molecules after annealing at 300 K for 1.25 ps. At this point ( $t = 0$ ) a first reducing electron is added to the system. (b) The formation of a linear  $\text{PtCl}_2^-$  complex upon reduction is completed ( $t = 2.2$  ps). Soon after, a Pt–Pt bond forms between the complexes. (c) Optimized geometry of the Pt(I)–Pt(II) dimer after annealing and quenching ( $t = 3.5$  ps). At this point, a second reducing electron is added to the system, which is annealed at 300 K for 2 ps. (d) Final geometry of the Pt(I) dimer.

basis set and without imposing periodic boundary conditions.<sup>40–44</sup> The system remained in the dimer geometry of Figure 5d, with the slightly higher Pt–Pt distance of 2.93 Å. The coordinate set of the structure after this additional optimization is reported in Table 2. The  $3N - 6$  nonzero eigenvalues of the Hessian matrix associated with the final optimized geometry are all positive, implying that this structure corresponds to a potential energy minimum.

To further characterize the structure, we analyze the motion of the Pt(I)–Pt(II) and the Pt(I)–Pt(I) dimers during 3 ps of unconstrained dynamical simulation in the gas phase. In both cases, the initial Pt–Pt distance is 0.1 Å bigger than its equilibrium value. As expected, the systems oscillate freely around their minimum energy configuration. In particular, for each dimer, a good approximation of the bond vibrational frequency can be readily obtained from the observed oscillations

of the Pt–Pt distance. For the Pt(I) dimer, the resulting Pt–Pt oscillation frequency is  $176\text{ cm}^{-1}$ , i.e., a value close to the value  $170\text{ cm}^{-1}$  assigned to the Pt–Pt stretching mode of the  $[\text{Pt}_2\text{Cl}_4(\text{CO})_2]^{2-}$  ion.<sup>17</sup> In the case of the Pt(I)–Pt(II) dimer, the estimated Pt–Pt stretching frequency is  $106\text{ cm}^{-1}$ . This value is intermediate between the  $176\text{ cm}^{-1}$  value we obtain for the Pt(I)–Pt(I) dimer and the  $81\text{ cm}^{-1}$  frequency of the Pt–Pt stretching mode of Magnus's green salt  $[\text{Pt}(\text{NH}_3)_4][\text{PtCl}_4]$ ,<sup>47</sup> where two square-planar units formally containing a Pt(II) atom are linked along the  $z$  axes by a weak Pt–Pt interaction. We interpret this result as an indication that the Pt–Pt bond in the Pt(I)–Pt(II) dimer considered in this work is stronger than the typical bonding of Pt(II)–Pt(II) complexes.

(47) Adams, D. M.; Hall, J. R. *J. Chem. Soc., Dalton Trans.* **1973**, 1450–1453.

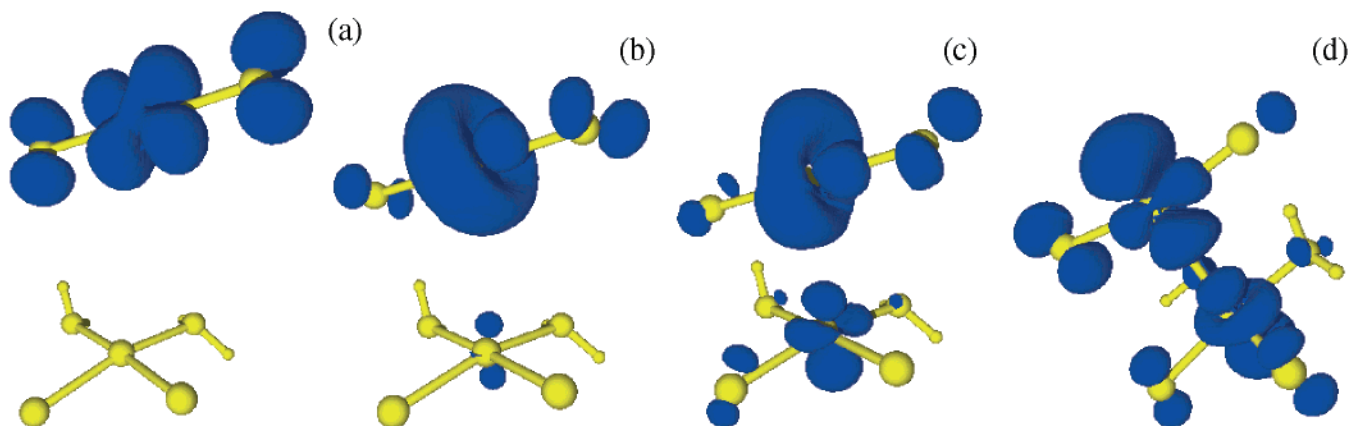


**Figure 5.** Evolution of the particle density associated with the unpaired electron during the formation of a Pt–Pt bond between a Pt(II) complex and a Pt(I) complex (isodensity surfaces at 0.002 au). (a–c) Results from the electronic structure optimization for three fixed gas-phase geometries. The Pt–Pt distances are 5.4 Å (a), 4.0 Å (b), and 3.3 Å (c). (d) Fully optimized geometry of the Pt(I)–Pt(II) dimer with the antibonding half-filled HOMO state. The equilibrium Pt–Pt distance is 2.9 Å.

**Table 2.** Final Geometry of the Pt(I)–Pt(II) Dimer Obtained in the Simulations after Adding One Electron to a System Containing Two  $PtCl_2(H_2O)_2$  Complexes<sup>a</sup>

atom	plane-wave basis set			Gaussian basis set		
	x (Å)	y (Å)	z (Å)	x (Å)	y (Å)	z (Å)
Pt(1)	3.741	1.997	1.938	3.907	2.081	2.138
Pt(2)	0.868	1.993	1.936	0.975	2.086	2.143
Cl(3)	4.121	3.636	3.486	4.360	3.354	4.092
Cl(4)	3.871	0.374	0.257	4.075	0.838	0.027
Cl(5)	0.424	3.118	3.859	0.463	3.205	4.168
Cl(6)	0.000	0.000	2.619	0.000	0.000	2.764
O(7)	1.032	1.005	0.082	1.157	1.156	0.251
O(8)	1.566	3.884	1.227	1.787	3.957	1.495
H(9)	1.490	4.391	2.080	1.665	4.578	2.262
H(10)	2.566	3.580	1.248	2.821	3.603	1.499
H(11)	2.033	0.758	0.000	2.147	1.027	0.000
H(12)	0.602	0.150	0.345	0.700	0.283	0.340

<sup>a</sup> The two coordinate sets are the result of two structural relaxations using a plane-wave basis set and a Gaussian basis set (see text, section IIID).

To further investigate the Pt–Pt bond, we use the theory of atoms in molecules originally introduced by Bader.<sup>48</sup> According to this theory, information about the chemical bonds in a molecule can be extracted from the topological analysis of the laplacian  $L = \nabla^2\rho$  of the (positive) electron density  $\rho$ . In transition metal complexes, the outer shell of the metal atom core presents zones of electron density depletion and accumulation, revealed by maxima and minima of  $L$ , respectively. These density distortions arise from the formation of bonds in the complex and reflect the geometrical disposition of the ligands.<sup>49</sup> We compute  $L$  for the Pt(I)–Pt(II) dimer, for the Pt(I)–Pt(I) dimer, and, as reference, for the  $[Pt_2Cl_4(CO)_2]^{2-}$  dimer. The isovalue surfaces of  $L$  at 0.03 au, representative of depletion regions, are presented in Figure 7. In the case of the Pt(I) dimers, two maxima of  $L$  are located along the Pt–Pt axes and the other maxima point toward the  $Cl^-$ , CO, and  $H_2O$  ligands (Figure 7b,c), as expected.<sup>49</sup> In the case of the Pt(I)–Pt(II) dimer, the laplacian presents a single maximum in the region between the Pt atoms, located close to the linear Pt(I) unit (Figure 7a), indicating a weaker chemical bond between the two metal atoms.

To summarize, a stable Pt(I)–Pt(II) dimer is obtained in the calculations. The topological analysis of the charge density

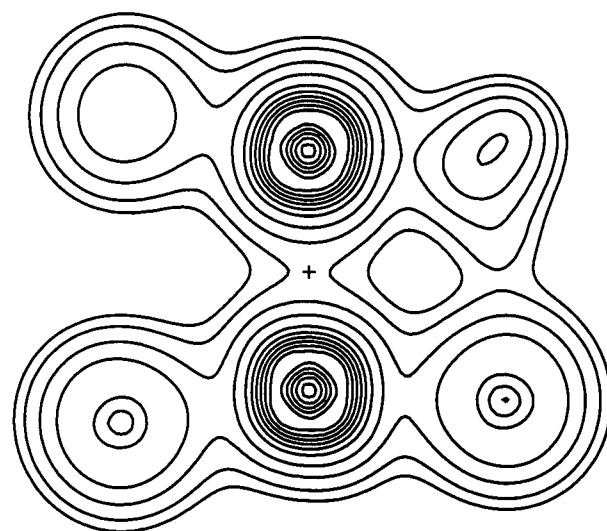


**Figure 6.** Contour plot of the electron density  $\rho$  of the Pt(I)–Pt(II) dimer  $[PtCl_2(H_2O)_2][PtCl_2^-]$  in the plane containing the two Pt atoms and one  $Cl^-$  ligand of the Pt(I) unit (right-bottom in the plot). The outer contour is at  $\rho = 0.0030$  au. The small cross indicates the (3,–1) bond critical point ( $\rho = 0.0054$  au) between the Pt atoms. On the right side, the hydrogen bond between a  $Cl^-$  ligand of the Pt(I) unit and a water ligand of the Pt(II) unit is visible (cf. Figure 5d).

(Figures 6 and 7), and the results concerning the bond distance, energy, and stretching motion, clearly indicate that a Pt–Pt bond forms between the two Pt complexes already after a single reduction step. The Pt–Pt interaction is then strengthened when an additional electron is acquired by the dimer during the second reduction step.

#### IV. Discussion

The electroless growth of platinum clusters in solution is a nucleation-dominated,<sup>13,50</sup> autocatalytic<sup>3,4,50</sup> process. The nucleation of platinum particles is generally believed to follow a two-step mechanism: (i) reduction of Pt(II) to isolated Pt(0) atoms and (ii) aggregation of the zerovalent atoms to form metal clusters. However, as we pointed out in the Introduction, there are experimental observations that cannot be explained by this nucleation model alone, like, e.g., the possibility of producing dimers which present higher oxidation states.<sup>17</sup> In addition, the

(48) Bader, R. F. W. *Atoms in Molecules—A Quantum Theory*; Oxford University Press: Oxford, 1990.

(49) Gillespie, R. J.; Bytheway, I.; Tang T.-H.; Bader, R. F. W. *Inorg. Chem.* **1996**, *35*, 3954–3963.

(50) Watzky, M. A.; Finke, R. G. *J. Am. Chem. Soc.* **1997**, *119*, 10382–10400.

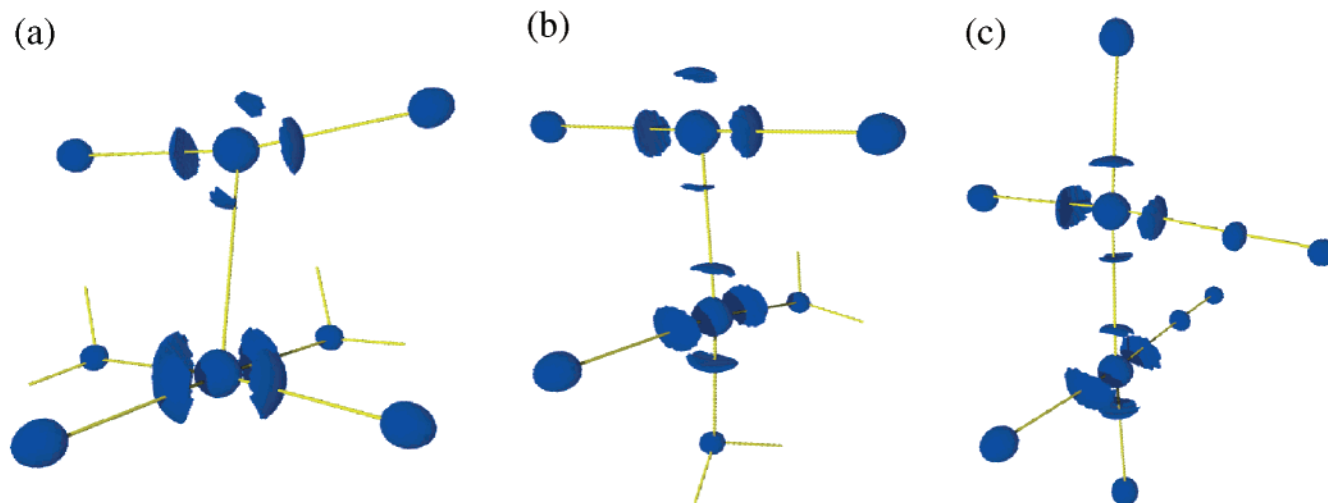


**Figure 7.** Isovalue surfaces of the laplacian of the electron density  $L = \nabla^2\rho$  at  $L = 0.03$  au for three platinum dimers. (a) The Pt(I)–Pt(II) dimer  $[\text{PtCl}_2(\text{H}_2\text{O})][\text{PtCl}_2]^-$  obtained in the simulations after adding one electron to a system containing two  $\text{PtCl}_2(\text{H}_2\text{O})_2$  complexes. (b) The Pt(I)–Pt(I) dimer  $\text{Pt}_2\text{Cl}_3(\text{H}_2\text{O})^-$  obtained after the addition of a second electron. (c) The Pt(I)–Pt(I) dimer  $[\text{Pt}_2\text{Cl}_4(\text{CO})_2]^{2-}$  (experimentally isolated in ref 17). One maximum of  $L$  between the Pt atoms in the Pt(I)–Pt(II) dimer (a) and two maxima between the Pt atoms in the Pt(I)–Pt(I) dimers (b,c) are evident, indicating that the metal–metal bond formed after the first reduction step is strengthened after the addition of a second reducing electron (see text and ref 49).

presence of Pt(0) atoms as reaction intermediates in the reduction of  $\text{PtCl}_4^{2-}$  with hydrogen leading to colloidal Pt particles has been recently ruled out.<sup>3</sup> The issue of determining the minimal reducing conditions sufficient to yield cluster nucleation is, furthermore, of great relevance to the closely related problem of achieving cluster growth on biological substrates. Indeed, such substrates may be used to drive heterogeneous cluster nucleation (competitive with the homogeneous processes taking place in the solution medium) if the reducing conditions are not too severe.<sup>6</sup> In the present work, first principles simulations are used to investigate the initial stages of the homogeneous cluster formation process. In a series of FPMD simulations, we observe the formation of a Pt–Pt bond after the reduction from Pt(II) to Pt(I) of a single Pt complex. The result is obtained both in the gas phase and in solution, starting from different initial conditions (varying, e.g., the relative position of the two complexes and the number and arrangement of the water molecules separating them). Within the predictive power of the DFT–GGA functional used, this is a sufficient condition to establish the existence of a novel reaction path to dimer formation in which, surprisingly, only *one* reducing electron is needed to initiate cluster formation, whereas *four* would be needed in the standard mechanism. By addition of a further electron, a Pt(I) dimer is obtained, which closely resembles the Pt dimer experimentally obtained upon reduction of  $\text{K}_2\text{PtCl}_4$  with CO in HCl solution.<sup>17</sup> We note that acquiring the necessary statistics to estimate the equilibrium constants of these reactions would far exceed the reach of current FPMD techniques. However, the microscopic mechanism provided by our simulations suggests a simple and consistent picture within which to interpret the existing experimental evidence. In the following, we discuss the nucleation process which in the standard experimental procedures leads to the formation of colloidal nanoparticles, taking in account the possibility of forming metal–metal bonds after the first reduction step.

**A. Role of the Hydrolysis in the Reduction Process.** It is known that the reduction of  $\text{PtCl}_4^{2-}$  is faster when the solution has been aged to allow the water substitution of one or two chlorine ligands, according to the reactions 1 and 2.<sup>4</sup> Thus, hydrolysis facilitates in some way the electron transfer from

the reducing agent to the metal complexes. The investigation of the electron-transfer mechanism is beyond the scope of this work. Consistent with the experimental observations, we may assume that electrons are transferred to the Pt(II) metal complexes only after hydrolysis. Our gas-phase electronic structure calculations support this assumption, giving a positive VEA only for the hydrolyzed diaqua complex  $\text{PtCl}_2(\text{H}_2\text{O})_2$ .

**B. Reduction of a Pt(II) Complex to the Monovalent and Zerovalent State.** In all our simulations, both in the gas phase and in water solution, the addition of one electron to  $\text{PtCl}_2(\text{H}_2\text{O})_2$  leads to a well-characterized linear Pt(I) complex  $\text{PtCl}_2^-$ . The  $\text{PtCl}_2^{2-}$  complex, where the Pt(0) atom is in the  $d^{10}$  electronic configuration, is obtained both by adding one further electron to  $\text{PtCl}_2^-$  and by adding two electrons to  $\text{PtCl}_2(\text{H}_2\text{O})_2$  at one time. We note that many examples exist of two-fold-coordinated linear complexes of transition metal atoms in the  $d^{10}$  electronic configuration, e.g.,  $\text{Hg}(\text{CN})_2$ ,  $\text{Au}(\text{NH}_3)_2^+$ , and  $\text{AgCl}_2^-$ .<sup>35</sup> In addition, whereas, to our knowledge, no examples of complexes containing one Pt(I) atom have been reported, linear Pt(0) $\text{L}_2$  complexes, where L is generally a phosphine, are known.<sup>51</sup> Phosphines are able to stabilize Pt(0) atoms through the overlap of their lone pair with the empty 6s Pt orbital, whose associated energy level raises relative to the 5d level if the atom is complexed.<sup>52</sup> Chlorine ligands, however, are not really effective in stabilizing atoms of late transition elements in low oxidation states,<sup>1</sup> so that the  $\text{PtCl}_2^{2-}$  complexes presumably cannot survive for a long time in the solution. This may explain why they have not been reported experimentally as stable species. If  $\text{H}_2\text{O}$  and  $\text{Cl}^-$  are the only available ligands (e.g., in the present case of a  $\text{K}_2\text{PtCl}_4$  solution), Pt(0) has been experimentally reported only in the form of metal particles. The Pt(I) and Pt(0) dichloro complexes  $\text{PtCl}_2^-$  and  $\text{PtCl}_2^{2-}$  should be thus thought of as metastable reaction intermediates. Interestingly, during the simulations it was always the water ligands

(51) Otsuka, S.; Yoshida, T.; Matsumoto, M.; Nakatsu, K. *J. Am. Chem. Soc.* **1976**, *98*, 5850–5858.

(52) Low, J. J.; Goddard, W. A., III. *J. Am. Chem. Soc.* **1984**, *106*, 6928–6937. Obara, S.; Kitaura, K.; Morokuma, K. *J. Am. Chem. Soc.* **1984**, *106*, 7482–7492. Noell, J. O.; Hay, P. J. *J. Am. Chem. Soc.* **1982**, *104*, 4578–4584. Balazs, A. C.; Johnson, K. H.; Whitesides, G. M. *Inorg. Chem.* **1982**, *21*, 2162–2174.



and never the chlorine ones which were observed to dissociate upon reduction of the  $PtCl_2(H_2O)_2$  complex. After this, the dichloro complexes remained stable for all the time of the MD simulations, and no water substitution was observed. These results indicate that the Pt atom in the  $d^9$  and in the  $d^{10}$  electronic configurations is better stabilized by chlorine than by water.<sup>53</sup> We note that this does not exclude the possibility of water/chlorine exchanges, which are certainly possible on the experimental time scale, inaccessible to our simulations. Indeed, the linear dichloro complex  $AgCl_2^-$ , very similar to  $PtCl_2^{2-}$ , is known to undergo partial hydrolysis.<sup>54</sup> However, it is a reasonable assumption that, for a fairly long time since the beginning of the reduction, negatively charged Pt(I) and Pt(0) linear dichloro complexes are present in the solution.

**C. Formation of the First Pt–Pt Bonds.** After some of the Pt(II) complexes are reduced to Pt(I), the nucleation of clusters may take place by various mechanisms, namely (i) further reduction to Pt(0) and formation of bonds with other zerovalent atoms; (ii) formation of bonds with other Pt(I) complexes; and (iii) formation of bonds with Pt(II) complexes. The first mechanism corresponds to the classical nucleation model, while the second is reminiscent of a reaction mechanism which has been proposed to explain the formation of Pt(I) dimers after reduction of platinum salts in solution.<sup>18</sup> The third mechanism is the one suggested by the results of the present work. In the case of  $K_2PtCl_4$ , we expect both the first and the second mechanisms to be limited by a further hydrolysis of the reduced complexes. Hydrolysis is necessary since reactions between negatively charged complexes would otherwise have to occur which are presumably hindered by long-range repulsive electrostatic forces. As discussed in the former section, the hydrolysis of  $PtCl_2^-$  or  $PtCl_2^{2-}$  never occurred in the simulations, so that these processes are likely to be associated with non-negligible energy barriers. As a consequence, both the first and the second mechanisms imply an activation energy for the nucleation of the cluster.

On the other hand, the reaction between  $PtCl_2^-$  and  $PtCl_2(H_2O)_2$  occurs spontaneously within a few picoseconds in our room-temperature simulations. This indicates that when a reducing agent is added to an aged solution of  $K_2PtCl_4$ , and as soon as a Pt(II) complex is reduced to Pt(I), there is a reaction path leading to a Pt–Pt bond which does not require an appreciable activation energy and does not imply bonding of negatively charged complexes. We thus think that this reaction may play an important role in the formation of Pt dimers, and more generally in the nucleation of Pt colloidal particles.

**D. Formation of a Pt(I) Dimer.** In our simulations, after a bond between a Pt(II) complex and a Pt(I) complex is formed, the addition of a further electron leads to a Pt(I) dimer after the loss of a chlorine ligand. Some indirect evidence of the existence of a Pt(I) dimer intermediate in the reduction of a  $K_2PtCl_4$  solution is related to one of the first isolated monovalent platinum dimers,<sup>17</sup> the  $[Pt_2Cl_4(CO)_2]^{2-}$  ion. This complex, structurally very similar to the Pt(I) dimer obtained in our simulations, can be produced with a method which closely resembles the standard colloid preparation, when a suspension of the  $K_2PtCl_4$  salt in concentrated hydrochloric acid solution is stirred with carbon monoxide at atmospheric pressure.<sup>17</sup> The main difference between this procedure and the standard preparation of colloids lies in the high concentration of  $Cl^-$  ions and in the presence of CO (the latter being both a reducing

agent and a stabilizing ligand for platinum). In these conditions, further reduction and growth accompanied by loss of the ligands is simply not possible, because of the strong metal–CO interaction and the high concentration of  $Cl^-$  ions present in solution. However, if extracted from the solution and dipped in water, the dimeric salt is not stable, and a black precipitate is obtained, which is presumably formed by aggregation of metallic particles.<sup>17</sup>

Thus, the preparation of  $[Pt_2Cl_4(CO)_2]^{2-}$  may be seen as a reduction process “frozen” at an intermediate step by the presence of stabilizing ligands in sufficient concentration, which would otherwise proceed until colloidal particles are formed.

**E. Growth of Colloidal Particles.** When no stabilizing ligands are present in the solution, a dimer represents an intermediate step toward the growth of bigger clusters. In particular, in the earliest stage of the reduction process, the concentration of unreduced Pt(II) ions is much higher than that of the reduced complexes. If the reduction rate is not too high, the formation of a bond between Pt(II) and Pt(I) complexes, which according to our results does not imply an activation energy, is thus a likely event. Once the Pt(II)–Pt(I) bond is formed, our results indicate that the addition of a second electron can promote the loss of a chlorine ligand (cf. Figure 4d). This way, the negative charge localized on the dimer is not increased when the formal valence state of the whole complex is reduced.

An iterated reduction/dechlorination mechanism could be important in the following stages of the reaction, favoring the reduction while the cluster grows by addition of Pt atoms which can be in a reduction state higher than zero. This model growth mechanism is related to what we observe in our calculations, where a bond forms between a Pt(II) atom in the stable  $d^8$  electronic configuration and a second Pt atom in the unstable open-shell  $d^9$  electronic configuration. Trying to generalize this result, we can speculate that similar reactions may happen at the surface of an open-shell cluster, playing the role of our  $d^9$  Pt atom. This would imply that not only is the addition of reduced Pt(0) atoms to a growing cluster possible, but also that of unreduced Pt(II) ions. The following reduction to the zerovalent state requires an electron exchange between the reducing agent and a whole cluster. This is favored, since due to the delocalization of the metallic orbitals the electron affinity of the cluster is higher than that of the single Pt atom complex.<sup>1</sup> This is consistent with the autocatalytic nature of the reduction process,<sup>50</sup> in which the presence of already formed clusters catalyzes the reduction of Pt(II) complexes.<sup>3–5</sup>

A key point of the present model is the formation of a Pt(I) complex reaction intermediate. We note that the existence of a Pt(I) intermediate has already been postulated<sup>11</sup> in the context of the sonochemical reduction of  $PtCl_4^{2-}$  to colloidal platinum.<sup>55</sup> Additionally, when Pt(II) is reduced by hydrogen, a mechanism where Pt(I) is the first intermediate can explain well the kinetics of the whole reduction process.<sup>3</sup> In the mechanism proposed in the present work, the Pt(I) complex provides the starting point for the autocatalytic growth of the metallic cluster. That is, every Pt(II) complex which receives one electron from the reducing agent and is reduced to Pt(I) can be a nucleation center for the growth of platinum particles. This is in agreement with the

(53) Similarly, an adsorbed layer of chlorine ligands is always present on the surface of colloidal Pt(0) metal particles.<sup>1</sup>

(54) Alexander, A.; Ko, E. C. F.; Mac, Y. C.; Parker, A. J. *J. Am. Chem. Soc.* **1987**, *89*, 3703–3712.

(55) Similarly, it has been suggested that the electrochemical reduction of Pt(IV) on graphite involves the formation of a Pt(III) intermediate (Zubimendi, J. L.; Vázquez, L.; Ocón, P.; Vara, J. M.; Triaca, W. E.; Salvarezza, R. C.; Arvia, A. J. *J. Phys. Chem.* **1993**, *97*, 5095–5102).

experimental observation that, in most reduction methods, the formation of metal particles is a nucleation-dominated process.<sup>13,50,56</sup>

The growth process is expected to continue at least until a closed-shell configuration is reached. Indeed, the size distributions of monocrystalline colloidal particles of transition metals are often determined by series of *magic numbers* of atoms in the cluster corresponding to atomic and electronic closed-shell configurations.<sup>12</sup> If the reduction rate is not too high, the growth is expected to proceed by addition of unreduced complexes. On the other hand, if a very high number of reducing electrons are available, the complete reduction to Pt(0) may presumably occur before the aggregation of atoms starts, as in the classical nucleation model. We note that a mechanism similar to the one proposed here has been proposed<sup>15</sup> to explain the nucleation of clusters upon radiolytic reduction of monovalent ions such as Ag<sup>+</sup> and Au<sup>+</sup>. Formation of dimers after aggregation of reduced Ag(0) atoms with excess Ag<sup>+</sup> ions as well as addition of monovalent ions to growing clusters has been observed.<sup>15</sup> According to our FPMD results, bivalent platinum ions can also form dimers after a single reduction step, suggesting that this may be a more general property of late transition metals.

## V. Summary

In a series of FPMD simulations, we observe a reaction mechanism leading to the formation of a Pt(I) dimer after reduction of K<sub>2</sub>PtCl<sub>4</sub> in aqueous solution. In a simulation cell

(56) Zoval, J. V.; Lee, J.; Gorer, S.; Penner, R. M. *J. Phys. Chem. B* **1998**, *102*, 1166–1175.

filled with water molecules to model the solution environment, one electron is added to two PtCl<sub>2</sub>(H<sub>2</sub>O)<sub>2</sub> complexes. The reduction of one of the square-planar complexes proceeds by loss of both water ligands, whereas the chlorine ligands move far away from each other until a linear PtCl<sub>2</sub><sup>-</sup> complex is formed. The reduced Pt(I) complex is able to react with the unreduced Pt(II) complex, forming a Pt–Pt bond along the *z* axes of the square-planar complex. The addition of a further electron promotes the loss of a chlorine ligand, and a Pt(I) dimer is obtained.

We suggest that the formation of metal–metal bonds between complexes in oxidation states higher than zero is a key step in the nucleation mechanism of colloidal particles upon reduction of platinum salt. Addition of unreduced complexes to growing clusters with an open-shell electronic configuration should also be possible. This way, the complete reduction to the zerovalent state involves the whole cluster, which has greater electron affinity than a monatomic complex. This is consistent with the autocatalytic and nucleation-dominated nature of the growth process of platinum nanoparticles.

**Acknowledgment.** The authors are grateful to F. Finocchi and T. Albaret for their help with the implementation of the spin-polarized DFT in the LAUTREC code, and to F. De Angelis for his help with the calculations involving Gaussian basis sets. The computing resources required for this study were provided by the Center for High Performance Computing at the Dresden University of Technology.

JA002977+